

## On the use of multi-resolution satellite image time series to detect land-cover modifications

Francois PETITJEAN<sup>†</sup>, Jordi INGLADA<sup>\*‡</sup> and Pierre GANÇARSKI<sup>†</sup>

<sup>†</sup>LSIIT/University of Strasbourg, UMR 7005, 67412 Illkirch Cedex, France

<sup>‡</sup> CNES/CESBIO, UMR 5126, 31401 Toulouse Cedex 9, France

(31 August 2012)

Upcoming temporal and spatial HR satellites such as Ven $\mu$ s, SENTINEL-2 and Landsat Data Continuity Mission (LDCM) will provide very valuable data for land-cover and vegetation monitoring. However, due to cloud cover and even to some rapid changes, a higher temporal resolution may be needed for some applications. In this work, we propose to use the higher temporal resolution of satellites with mid- to low- spatial resolutions such as upcoming PROBA-V. The aim of this work is to study how images provided by satellites with a lower spatial resolution but with a higher temporal one, can be used in order to get information about the temporal classification derived from Satellite Image Time Series (SITS) provided by high resolution satellites such as Ven $\mu$ s, SENTINEL-2 or LDCM.

We show that the low spatial resolution SITS can be used in order to inform about the stability and relevance of the high spatial resolution classification. Experiments include a wide variety of resolution ratios and study the use of each ratio from global to class-specific invalidation of the high resolution classification map (computed from the high spatial resolution SITS).

This work contributes to the assessment of the usefulness of the joint use of PROBA-V data and Ven $\mu$ s/Sentinel-2/LDCM images for land-cover monitoring.

### 1. Introduction

Upcoming temporal and spatial HR satellites such as Ven $\mu$ s, SENTINEL-2 and Landsat Data Continuity Mission (LDCM) will provide very valuable data for land-cover and vegetation monitoring. The 2- to 16-day revisit cycle and 10 to 30 meter resolution is particularly useful. However, due to cloud cover and even to some rapid changes, a higher temporal resolution may be needed for some applications.

One of the ways to improve the temporal resolution for these satellites is to merge their data with higher temporal resolution systems. For now, these other systems will fatally have a lower spatial resolution or a limited field of view.

Past research works have developed fusion approaches for using the synergy between HR resolution and mid- to low-resolution images. One of the conclusions of these works was that the resolution ratio between the images to fuse need to be not too far apart (Inglada *et al.* 2011). The increased resolution of PROBA-V with respect to the SPOT-VÉGÉTATION sensor seems to be well suited for this kind of applications.

The goal of this work is to propose a method to exploit the complementarity between Satellite Image Time Series (SITS) of different resolutions in order to provide up to date information about land-cover for every new available acquisition it being low or high resolution. One very original contribution of this work is the possibility

---

\*Corresponding author. Email: [jordi.inglada@cesbio.cnes.fr](mailto:jordi.inglada@cesbio.cnes.fr)

of providing a *degree of doubt* for the obtained classification, which makes it possible to detect incoherencies between the high resolution and the low resolution SITS.

This work contributes to the assessment of the usefulness of the joint use of PROBA-V data and Ven $\mu$ s/SENTINEL-2/LDCM images for land-cover monitoring.

## 2. High and low resolution satellite image time series: supplementary data

### 2.1 Context

As stated previously, recent satellites are able to sense high resolution SITS with a high revisit time (*i.e.*, with a high frequency of the temporal sampling). The data that will be produced opens up a number of new opportunities for the detailed analysis of temporal behaviours of evolution. For example, SENTINEL-2 will provide an observation of the same scene every ten days with spatial resolutions from 10 m to 60 m (moreover, a second identical satellite will be launched one year later in order to reduce the revisit delay by 50 %). One of these opportunities corresponds to the quasi real-time production of land-cover maps, in order to finely describe – for example – agricultural practices (Inglada and Garrigues 2010)<sup>1</sup>. However, even with these new sensors – and depending on the considered application – the temporal sampling frequency can be insufficient. Actually, even if the maximum number of images is acquired – with regard to the satellite revisit time – the cloud-covering of sensed scenes may sharply reduce the temporal sampling of geographic areas  $(x, y)$ . In our previous work (Petitjean *et al.* 2012b), we showed how a particular similarity measure – namely Dynamic Time Warping (DTW) – can be used in order to take into account the whole set of clear pixels, without removing neither too cloud-covered images nor cloud-contaminated temporal profiles. However, even if DTW makes it possible to exploit all available information about the sensed surface, the temporal sampling of the resulting radiometric series can still be insufficient depending on the considered application and sensed area.

Based on this observation – and as we can't influence neither the revisit time of the satellite nor the cloud-covering – the only way to obtain any intermediate information between two clear pixels from a radiometric series is to use data sensed by other sensors. In this context of heterogeneous SITS analysis, we focus here on the use of low-resolution images, which are usually sensed by daily revisiting satellites. For example, MODIS is sensing images with spatial resolutions from 250 m to 1 km, with a daily revisit time.

Our aim is thus to take the most of low/high spatial resolution images, with regard to the usual corresponding temporal sampling difference: high spatial resolution images (HR) provide a detailed information about the sensed surface-state at several dates, while low resolution images (LR) provide a frequent information on the radiometric evolution of the scene but with a coarse spatial resolution<sup>2</sup>.

### 2.2 State of the art

The use of this LR/HR complementarity for automatic SITS analysis actually began quite recently. Two main families of methods can be distinguished.

---

<sup>1</sup>An example requiring a high sampling frequency corresponds to the distinction between winter wheat crop and silage winter wheat crop. The last one actually differs from the first only by the harvest date, which occurs a little sooner (before complete maturation). The two harvest dates can actually be sufficiently close to require a high temporal sampling to differentiate them.

<sup>2</sup>As a consequence of the coarse spatial resolution, the radiometric information is also less accurate to distinguish several land-cover types. Actually, by sensing wider unit areas, LR images are also mixing more spectral signature within a single pixel.

The first family consists of synthesising HR images from LR ones, in order to provide a homogeneous SITS to the classification algorithm. In this way, each LR image is replaced by a fused HR image, usually using the closest (in time) HR images in the series. Laporterie and Flouzat (2003), Laporterie-Dejean *et al.* (2004) initiated this solution and proposed to fuse the LR images between two HR images with a morphological pyramid. Following the same idea, Inglada *et al.* (2011) studied several fusion strategies for the production of land-cover maps. However, these methods based on the fusion of the images are making strong hypotheses on a certain consistency/stability of objects composing the sensed scene between the LR and HR images that are fused. In this way, if the LR image is quite different from the closest HR image(s) – for instance if the harvest happens between the HR and LR images – the HR image that is synthesised from the LR one can be inexact.

The above-mentioned hypotheses on the comparability between two sensed images led the researchers to a second family of methods that are trying to reconstruct a HR information from LR results (opposed to previous methods that are modifying the data before the classification step). In this way, Gupta (2011) proposed to separately classify every image (LR and HR) of the series, then to manually fuse the several produced maps, in order to produce urbanisation maps. This approach is however quite limited due its manual step. In a more automatic way, Chen *et al.* (2002) proposed to use the precision of the SPOT VÉGÉTATION sensor (spatial resolution  $\sim 1$  km) in order to improve an AVHRR (spatial resolution  $\sim 2, 5$  km) model for the production of vegetation maps. Yang and Lo (2002) proposed to separately classify each image and then to study *a posteriori* differences for change detection, using the geographic coordinates of the pixels for the mapping of the classification maps. The proposed methodology belongs to this family of methods, and aims at not making any assumption about the consistence between HR and LR images. Our aim is to provide an intermediate information between two HR images about the ongoing evolution of the sensed area.

Finally, at the edges of this state of the art about the use the complementarity between HR and LR images, we would like to mention our recent work (Petitjean *et al.* 2012a), which is in line with the handling of multi-resolution SITS in the specific context of SITS composed of couples panchromatic/multi-spectral. This work proposes to enrich the radiometry of the pixels by geometric features (*e.g.*, area, compacity). Even if the proposed methodology was validated on multi-spectral SITS only, its relevance would be particularly improved by computing the spatial features on the panchromatic image of each couple. As stated previously, this work is however limited to this kind of data and does not address the current aim of using the HR/LR complementarity in terms of the temporal sampling and radiometric description.

### 2.3 Line of work

The aim of our proposal is to provide an updated information at every new sensed image – whether LR or HR – in order to handle the stream of information describing the SITS-observed area. To this end, we propose to use the HR stream to provide a reference classification, and the LR stream to describe the intermediate surface-state between two HR images. The underlying idea is that LR images do not provide the same accuracy than HR images for the classification step, but are providing a useful information with regard to the evolution of the scene between two HR images.

Contrary to approaches developed by F. Laporterie and by J. Inglada, we focus here on the use of the intermediate LR information without any pre-fusion of the data. We particularly focus on the use of LR images in order to invalidate part or totality of the HR temporal classification.

### 3. An on-line algorithm for classification’s reconsideration

#### 3.1 Principle

The aim of the proposed approach for the use of LR images composing a multi-resolution SITS, is to provide an intermediate information between to HR images. By “waiting” an up-to-date HR image, the proposed approach aims at providing a confidence information about the HR clusters of the classification built from the current HR-SITS. To this end, we consider the two LR and HR SITS separately, without inserting LR images into the HR SITS. The underlying idea is to give information about the necessity to acquire a new HR image and/or to trigger and guide the field campaigns. The proposed method is an on-line approach, *i.e.*, providing an updated information throughout both HR and LR streams. It makes it possible to provide a confidence information on the clusters of the temporal HR classification, for every new LR image arrival. The proposed approach is based on the analysis of the distribution of each HR temporal cluster of evolutions with regard to the LR ones.

Please note that *cluster* is used here in a general manner to denote both supervised and unsupervised classes. The proposed approach will actually be illustrated with an unsupervised classification algorithm, in order to avoid the bias introduced by the choice of learning samples and thus to be able to focus on the core of the framework. Nevertheless, the proposed approach could also be used with a supervised algorithm.

Let us exemplify our approach with two winter crops: barley and winter wheat (their phenologies are illustrated in Figure 1). It can be noticed that one of the significant differences – enabling to distinguish them – corresponds to the harvest date: early in May for barley and end of May for winter wheat. Let’s suppose a mix-up between these two classes at time  $t$  just before the harvest, both in LR and HR. Corresponding HR fields will thus be part of the same LR cluster at time  $t$ . Then, let  $t + 1$  be the sensing time of the next LR image between these two harvests (with no HR image between  $t$  and  $t + 1$ ), both barley and crop classes will be distinguished in the LR classification (but the HR classification will remain unchanged since no new HR image is available at  $t + 1$ ). Then, the re-computed distribution of HR clusters into new LR ones will lead to a different distribution compared to the one computed at  $t$ . We propose to use this distribution difference to assess the relevance of HR clusters at  $t + 1$ .

#### 3.2 Formalisation

The proposed on-line algorithm is composed of three main steps:

- initialisation;
- processing the sensing of a new HR image;
- processing of the arrival of a new LR image.

We moreover suppose that a LR image is associated to every sensed HR image. In practice, this image could be either sensed by a LR satellite or be obtained by degrading the HR image.

**3.2.1 Initialisation.** The initialisation step aims at providing the reference distributions of HR clusters into LR ones. Therefore, a HR classification and a LR one have to be computed from the available data. The HR classification corresponds to the classification of the first image sensed over the considered sensing period. The LR classification corresponds to the LR SITS composed of all images sensed



(a)



(b)

Figure 1. Winter Wheat (a) and barley (b) phenologies computed from the HR SITS using the reference land-cover map for 2006.

until the first HR image of the series. Note that the classification of SITS is made using the Dynamic Time Warping similarity measure, see (Petitjean *et al.* 2012b) for a detailed explanation. Then, for each HR cluster of the HR classification, its distribution into LR clusters can be compute – in practice we propose to model the distribution by a composition histogram. We use the geographic coordinates to map LR and HR areas.

This operation allow us at time  $t_0$ , where the proposed algorithm starts, to provide a distribution histogram of every HR cluster  $c$  into LR ones. Let us note  $\mathcal{H}_t^c$  the distribution histogram of a HR cluster  $c$  into LR ones at time  $t$ . Then, the initial distribution histogram of a HR cluster  $c$  into LR ones corresponds is denoted by  $\mathcal{H}_{t_0}^c$ .

**3.2.2 Sensing of a new HR image.** The sensing of a new HR image corresponds to the re-initialisation of the algorithm. The procedure is thus similar to the initialisation step. The difference lies in the fact that the HR classification then consists of a classification of the HR SITS (and not of a single image anymore).

**3.2.3 Sensing of a new LR image.** This step is actually our main contribution for multi-resolution SITS analysis and corresponds to the inductive case, which allows us to provide an on-line algorithm. The aim is, starting from a reference state at time

$t_i$ , to provide a confidence information on the HR clusters at time  $t_{i+1}$  when a new LR image is sensed. To this end, the main idea is to compute the distribution of HR clusters into LR ones from the LR classification of the LR SITS including this new LR image. The confidence information about the stability of HR clusters between  $t_i$  and  $t_{i+1}$  will thus be obtained from the comparison between the two corresponding distributions (we use the Euclidean distance to compute this similarity) .

In practice, we have at  $t_i$ :

- a classification of the LR SITS, as well as its learning model;
- a classification of the HR SITS, as well as its learning model;
- a reference histogram  $\mathcal{H}_{t_i}^c$  representing the distribution of HR clusters into LR ones at this time  $t_i$ .

Our main hypothesis is that, having also the distribution histogram  $\mathcal{H}_{t_{i+1}}^c$  of HR clusters into LR ones at time  $t_{i+1}$ , if  $\mathcal{H}_{t_i}^c \sim \mathcal{H}_{t_{i+1}}^c$  then the HR cluster  $c$  would not have evolved much between  $t_i$  and  $t_{i+1}$ . Note that, for this similarity to be defined, histograms have to be comparable, *i.e.*, described on the same LR clusters. Then, LR clusters at time  $t_i$  have to match the ones at time  $t_{i+1}$ .

The computation of histogram  $\mathcal{H}_{t_{i+1}}^c$  then lies in the ability to keep an equivalence between LR clusters at  $t_i$  and the ones at  $t_{i+1}$ . To this end, the proposed method consists of classifying the LR SITS that includes the new LR image, with the learnt model on the LR SITS that excluded it (*i.e.*, at  $t_i$ ). Considering a classification model consisting of centroids or of labeled samples, we then use the ability of the Dynamic Time Warping (DTW) similarity measure to compare sequences with different lengths and samplings (as described in (Petitjean *et al.* 2012b)).

As a summary, when a new LR image is sensed, the proposed approach follows the process:

- (i) classification of the LR SITS that includes the new LR image, by using the classification model learnt without it;
- (ii) computation of the distribution histograms  $\mathcal{H}_{t_{i+1}}^c$  of every cluster  $c$  of the HR SITS classification into the clusters of the new LR SITS classification (at time  $t_{i+1}$ );
- (iii) characterisation of the confidence/stability of every HR cluster  $c$ , by evaluation the similarity between  $\mathcal{H}_{t_i}^c$  and  $\mathcal{H}_{t_{i+1}}^c$  (using the Euclidean distance);
- (iv) spatial mapping of the confidence of each HR cluster  $c$ , in order to provide a confidence map of the sensed area.

Finally, note that the radiometric levels of LR and HR images do not have to be comparable to each-other; only the semantic of the images have to be similar, *i.e.*, able to distinguish similar land-cover classes.

## 4. Material & method

### 4.1 Image data

We detail here the main information concerning the images used for this work. The area of study of this work is located near the town of Toulouse in the South West of France. There are 46 FORMOSAT-2 images acquired over the 2006 cultivation year. The temporal distribution of the studied SITS, as well as its cloud-covering are given in Figure 2 and one image of the series is given in Figure 3.

From these images, we use the multi-spectral product at a spatial resolution of 8 m and only the three bands Near-Infrared, Red and Green are kept, since the blue channel gives little information about vegetation and is very sensitive to atmospheric

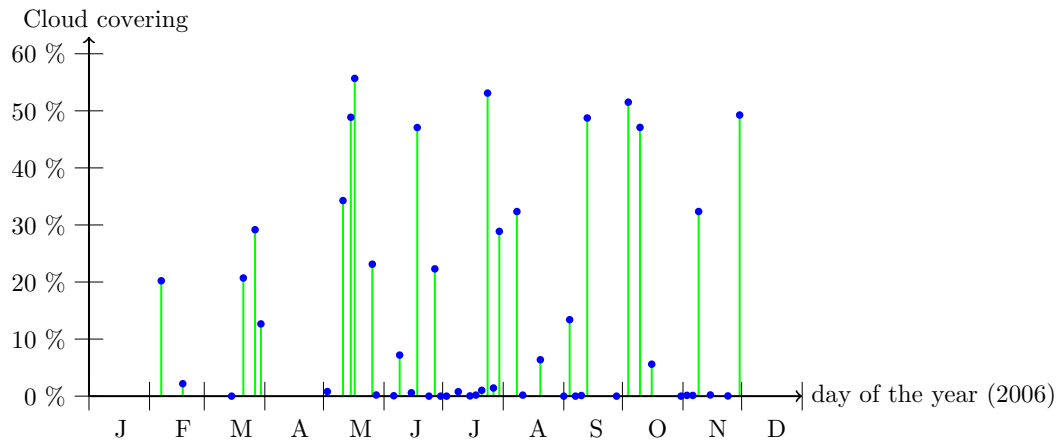


Figure 2. Cloud covering and temporal sampling of SITS used. Each spot represents a sensed image.

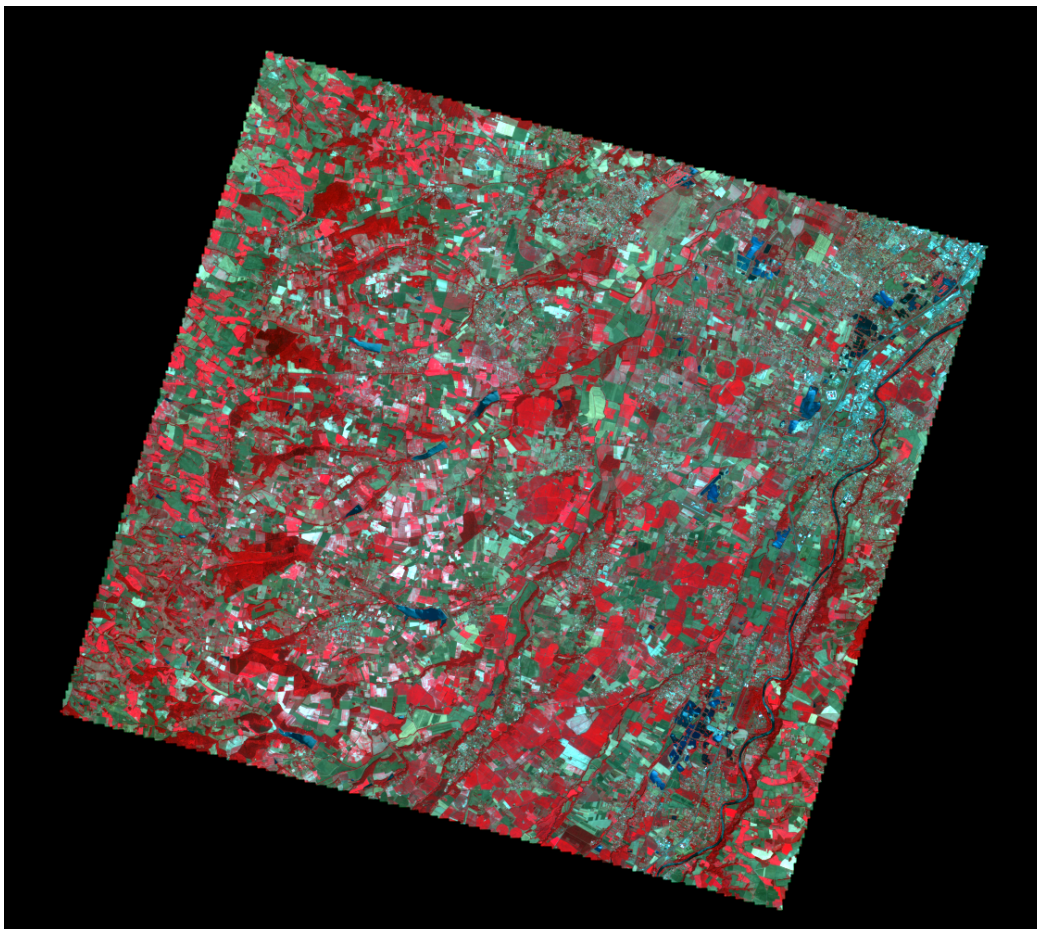


Figure 3. One image from the series (June, 29<sup>th</sup> 2006).

artifacts.

Before being used in this work, the FORMOSAT-2 products have been orthorectified (guaranteeing that a pixel  $(x, y)$  covers the same geographic area throughout the image series). All images also undergo processes in order to make the radiometric pixel values comparable from one image to another. These processes consist of converting the digital counts provided by the sensor into a physical magnitude and in restoring their own contribution to the surface by correcting for atmospheric effects. From the instrument radiometric model, digital numbers are first converted into

reflectances (normalized physical quantity of solar irradiance). The absolute calibration coefficients used in this step come from the monitoring of FORMOSAT-2 sensor conducted by the French Space Agency. The inversion of the surface reflectance is then made by comparing the measured reflectance in simulations at the top of the atmosphere, carried out for atmospheric and geometric conditions of measurement. The elevation is taken into account by carrying out simulations for various altitudes, including a weighting of the atmospheric pressure and the amounts of aerosols and water vapor. The state of the atmosphere at the time of the sensing is in turn characterised using meteorological sources (NCEP for the pressure and the humidity), using ozone data sources (TOMS or TOAST) and using aerosol data (SEAWIFS, AERONET). Otherwise, climatological values are used.

Moreover, for each cultivation year, we have a land cover map produced by the method described in (Idbraid *et al.* 2009) and using a comprehensive ground reference data set. Also, cloud masks are produced using the cloud screening procedure described in (Hagolle *et al.* 2010).

#### 4.2 Generation of the LR SITS

In order to be able to study the influence of the resolution ratio between the LR and the HR SITS, the LR images composing the LR SITS are generated from the HR images. The degradation (*i.e.*, zooming out) operator used to produce a LR image from a HR one corresponds to transformations based on a prolate spheroidal wave functions. For more information, the reader could refer to the work of Malgouyres and Guichard (2001) detailing the influence of five degradation operators.

Agronomic experts chose five HR images from the whole SITS to constitute the HR SITS: 14 March, 5 June, 29 June, 17 July and 27 September. These images were thematically selected in order to maximise the separability of the crop classes with five samples.

Regarding the LR images, the SITS composed of all 46 images has been generated for different spatial resolutions: 24 m, 32 m, 64 m, 96 m and 320 m, the latter being representative of the PROBA-V image resolution.

#### 4.3 Learning algorithm

We chose to use an unsupervised classification algorithm in order to validate our approach; the underlying idea is to avoid any bias that would be introduced by the choice of examples, and to focus on the ability to provide accurate confidence maps. To this end, we used the K-MEANS algorithm, both for the classification of LR and HR SITS. As we already stated, the distance used to compare temporal radiometric profiles is DTW and the corresponding averaging method introduced in (Petitjean *et al.* 2011). In this way, the LR SITS classification at  $t_{i+1}$  using the model learnt on the one at  $t_i$ , corresponds to a simple linking of each radiometric evolution to the closest centroid (DTW being able to compare sequences with different lengths and sampling). In order to guarantee that the LR learnt model fits the HR one, the LR model is only re-trained when a new HR image is sensed.

#### 4.4 Production of intermediate results – confidence

The proposed method allows us to provide, after every sensing of a new LR image, a confidence information about each HR temporal cluster since the last HR sensing. This information allow us to provide a map (HR) about the stability of HR clusters from the last HR sensing. Moreover, this confidence information can also be aggre-

gated in a general confidence on the classification, which can for instance give an information on the necessity to acquire a new HR image, when the confidence on the classification reaches a too low level.

In addition, as we work here with unsupervised classifications, it is also possible to map the confidence over the thematic clusters, by using the temporal reference classification map, in order to assess the relevance of the proposed approach.

## 5. Experiments

The validation assessment of the proposed method aims at evaluating its ability to handle streams of both LR and HR images. The HR SITS always corresponds to a spatial resolution of 8 m. The spatial resolution of the LR SITS will remain constant over the series; one simulation will be carried out for every resolution ratio (*e.g.*, 8 m – 24 m or 8 m – 96 m). The resolution couple 8 m – 24 m will provide reference simulation results ; the availability of this type of resolution is not *a priori* interesting with current satellites – since the revisit time of satellites providing 24 m images is usually similar to the one of satellites providing 8 m ones – but makes it possible to apprehend other results with regard to this reference one. Finally, note that confidence scores provided by the proposed method are normalised by the maximum theoretical distance between two distribution histograms, *i.e.*,  $\sqrt{2}$ .

The first study of the carried out simulations corresponds to the analysis of confidence maps produced at each arrival of a new LR image. Every map has been computed from the whole sensed area (24 km×24 km). An example of such a confidence map is illustrated in Figure 4; to ease the interpretation, we will however focus on a particular area, delimited by the square in the same figure.

The sets of (restricted) intermediate maps produced for the LR SITS with spatial resolutions of 24 m, 64 m and 320 m are respectively presented in Figure 5, 6 and 7. In a global manner, it can be noticed that the information provided by these three resolutions is quite similar, with an over-evaluation of the confidence with the decrease of the resolution. This gives a first quality trend on the relevance of the proposed method.

This visual remark is also statistically assessed, as illustrated in Figure 8. This figure presents the evolution of the global doubt on the classification – opposite of the confidence – with the number of days in the year 2006 (with time). Several comments can be made from this figure.

Firstly, the doubt on the HR classification increases between two HR acquisitions, which appears to be consistent. Indeed, going away from the last sensed HR image, the evolution probability of sensed areas increases. Note that this increase is progressive, which gives a first trend on the stability of the proposed approach.

Secondly, the doubt on the HR classification increases faster at the beginning of the year than afterwards. This behaviour is easily understandable: the HR classification of the SITS composed of a single image (at the beginning of the year) is less reliable than when the HR SITS is composed of a series of four or five images (at the end of the season).

Thirdly, we can see the same interpretation as the one visually made on the maps: the over-estimation of the confidence increases with the decrease of the resolution of LR images. This behaviour can be explained by samples that are more and more mixed since they are covering wider areas (and thus mixing up more atomic spectral signatures). Let us recall that a single pixel of a 320 m image covers 1 600 pixels of the HR image at 8 m spatial resolution; the description of the surface-state is thus necessarily coarser. In addition, it can be noticed that the order of the curves remains almost identical throughout the sensing year, which gives a second indication on the

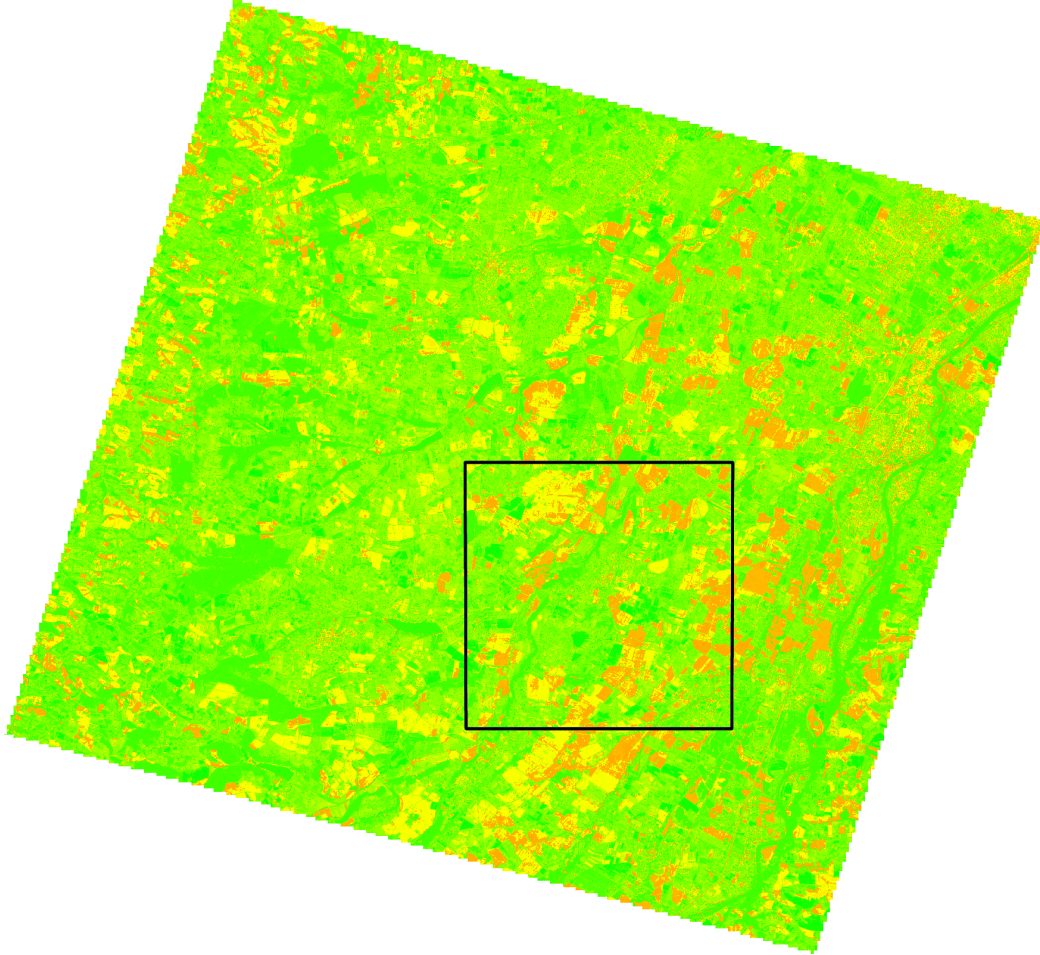


Figure 4. Confidence map produced for the arrival of the LR image of February, 29<sup>th</sup> 2006 during the simulation using the resolution ratio 8 m – 24 m. The confidence on the classification has been projected onto a “green to red” scale, green represents thus a good confidence on the classification while red corresponds to a high doubt on it. The delimited square corresponds to the crop on which interpretations will be detailed.

stability of the proposed process.

Fourthly, up to a scale factor, all simulations make it possible to assess the global confidence on the HR classification. This point is very important, since it allows us to show that LR images, even with a resolution of 320 m, can be used in order to help the expert in – for instance – the decision of acquiring a new HR image.

Fifthly, the main increases of the doubt correspond to surface-state changes of the main thematic classes. For example, the doubt increase between days 80 and 120 (*i.e.*, between end of March and early May) – even if there are accentuated by the low quality the HR classification that is only using a single image – corresponds to the growth of winter crops (*e.g.*, winter wheat). Similarly, the fast doubt increase between days 160 and 180 (*i.e.*, between mid-June and mid-July) corresponds to the growth of summer crops (*e.g.*, corn). Once these main steps of the agricultural season are over, it can also be noticed that the confidence then stays very high on the classification.

Figure 9 details the distribution of the doubt on the classification for the main thematic classes. It can be noticed that between the two first HR images, the doubt is quite important and also quite homogeneous; one can nevertheless note that the classification of forest areas is very uncertain, which can be explained by the growth of the leaves (bud break) over this time-period. The same comment can be made for winter crop classes. The doubt on summer crop classes comes from the gathering

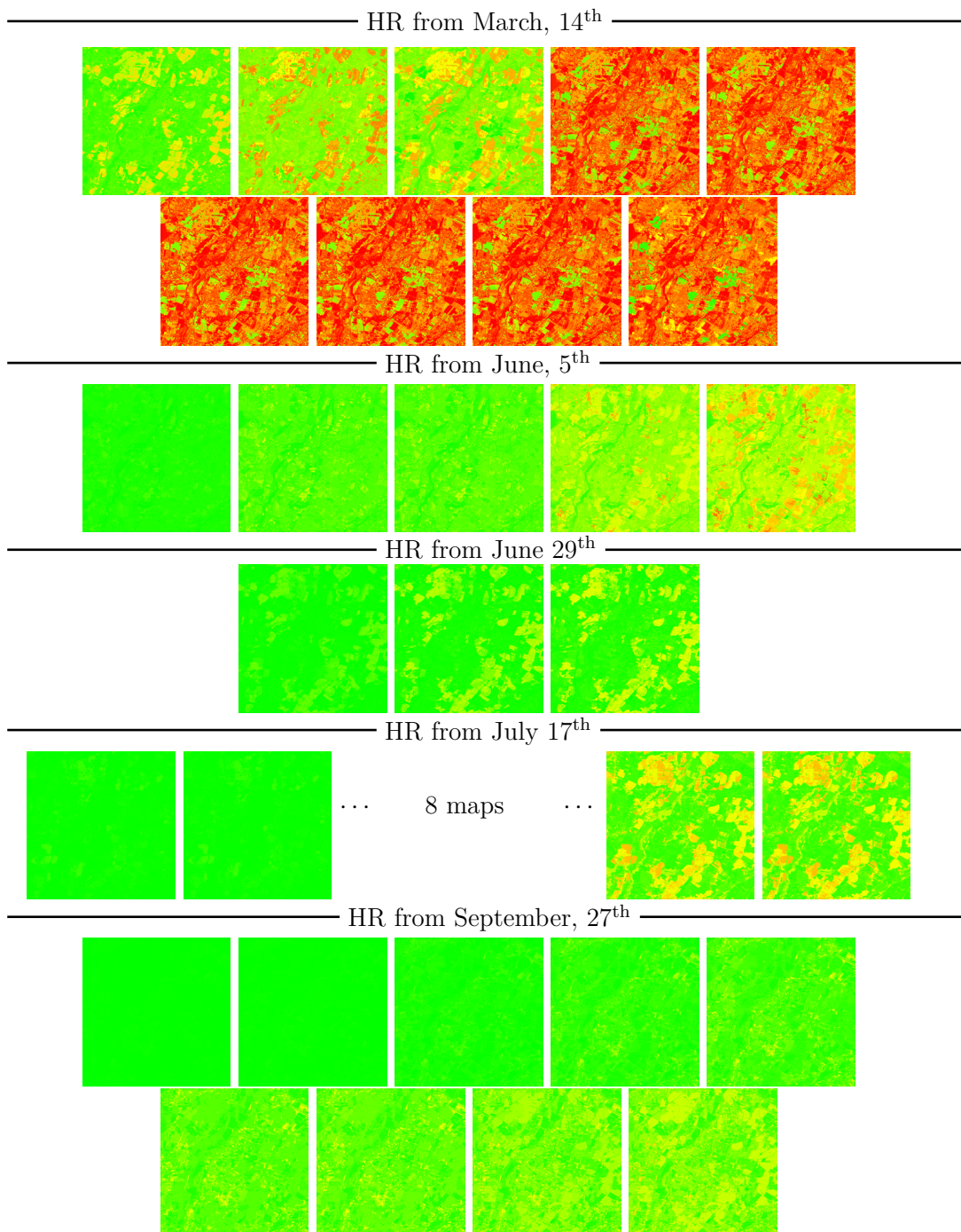


Figure 5. Set of confidence maps produced for a low spatial resolution of 8 m – 24 m. The confidence on the classification has been projected on a “red to green” scale. Every horizontal line represents the sensing of a HR image.

of summer and winter ones at this time, since the corresponding fields are both corresponding to bare soil in the beginning of the year. Regarding the water class, one can note that, once correctly classified, the corresponding doubt remains very low, which is quite consistent since water surfaces are not evolving much in the year.

Even if the evaluation accuracy of the confidence on the classification decreases with the used low spatial resolutions in the simulation process, one can still notice that class-by-class results for the simulation 8 m – 320 m remain quite consistent with regard to the different observed phenologies, even with such mixed pixels. For instance, one can see that after the harvest of winter crops (end of May), the doubt

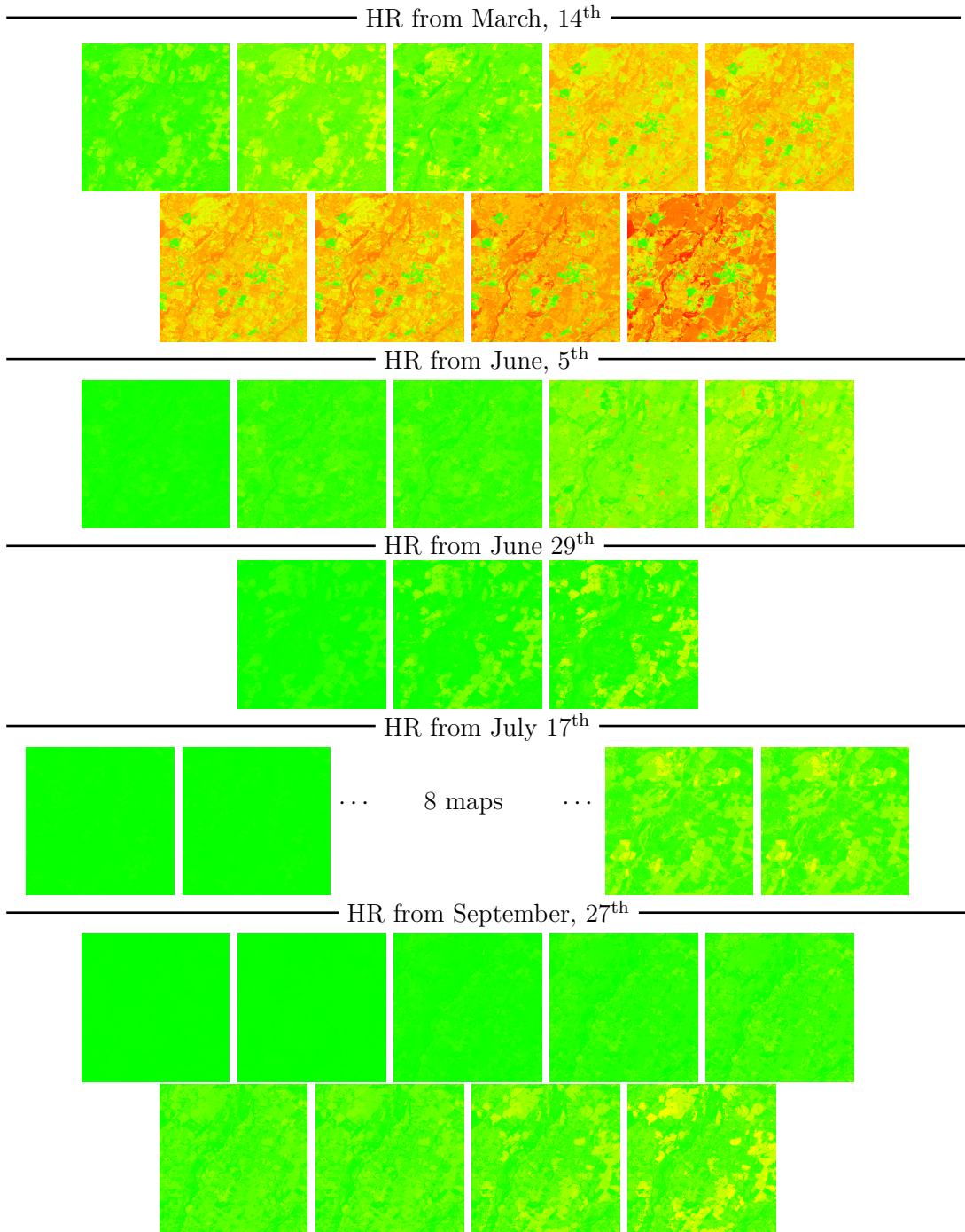


Figure 6. Set of confidence maps produced for a low spatial resolution of 8 m – 64 m.

associated to these parcels remains inferior to the one of summer crops.

Carried out experiments have shown that low spatial resolution images, sensed between two high resolutions images, represent a rich and exploitable information. We saw that, having close spatial resolution between LR and HR, the extracting information can provide a useful description of ongoing changes of the thematic classes. When the difference between low and high resolutions increases, we have seen that the global confidence on the classification can be as reliable as the one with the most favourable resolution ratio. This point indicates a possible future use of the Belgian PROBA-V satellite, which will provide daily images with a spatial resolution from 100 m to 300 m.

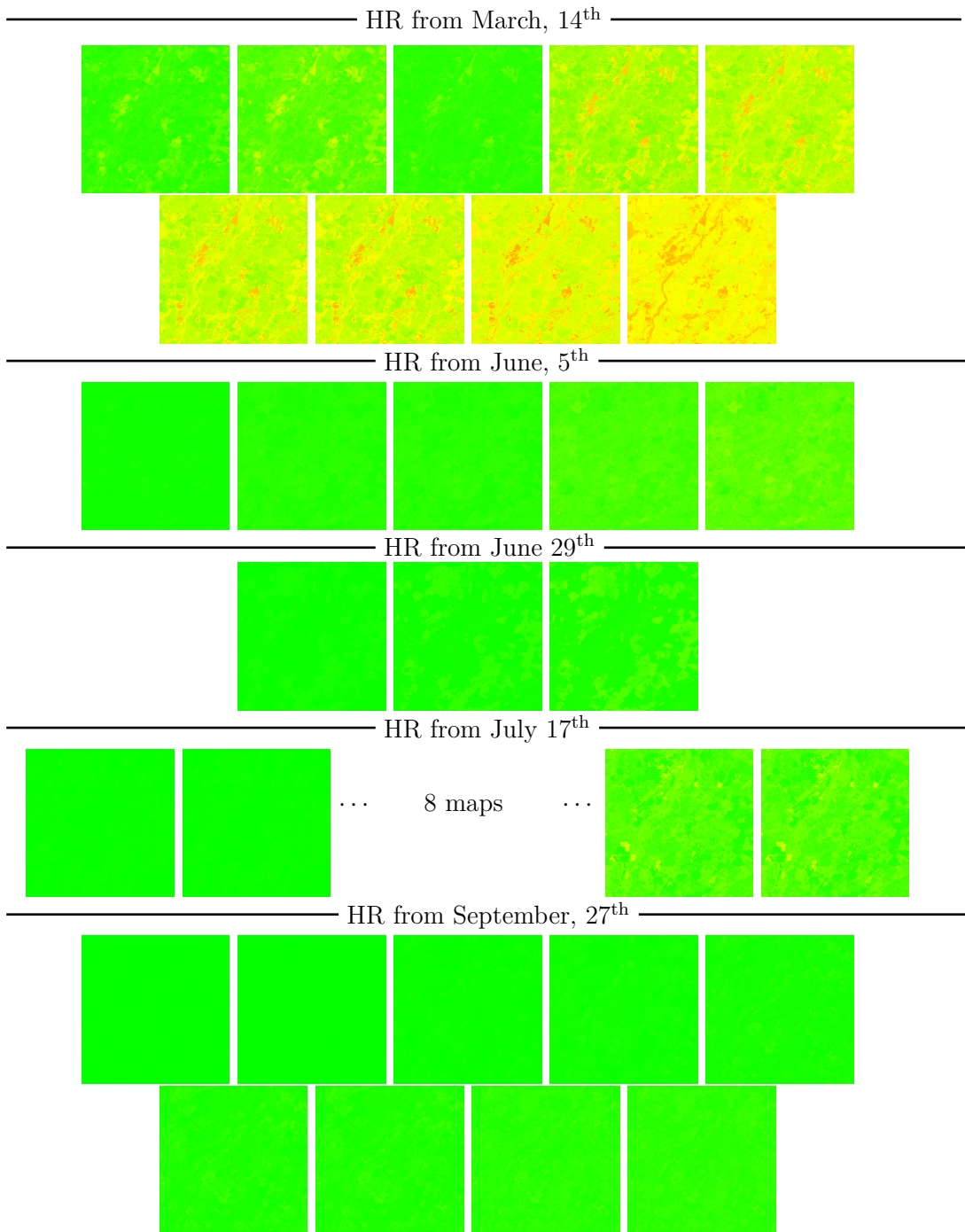


Figure 7. Set of confidence maps produced for a low spatial resolution of 8 m – 320 m.

## 6. Conclusion

The approach presented in this paper shows what can be achieved by the joint use of image time series of different spatial resolutions and constitutes an interesting contribution for the joint use of data from the coming PROBA-V mission together either with high spatial resolution systems either existing as Landsat or soon to come as SENTINEL-2.

Carried out experiments have shown that low spatial resolution images, sensed between two high resolutions images, represent a rich and exploitable information, both for global or class-specific assessment of the HR-SITS classification.

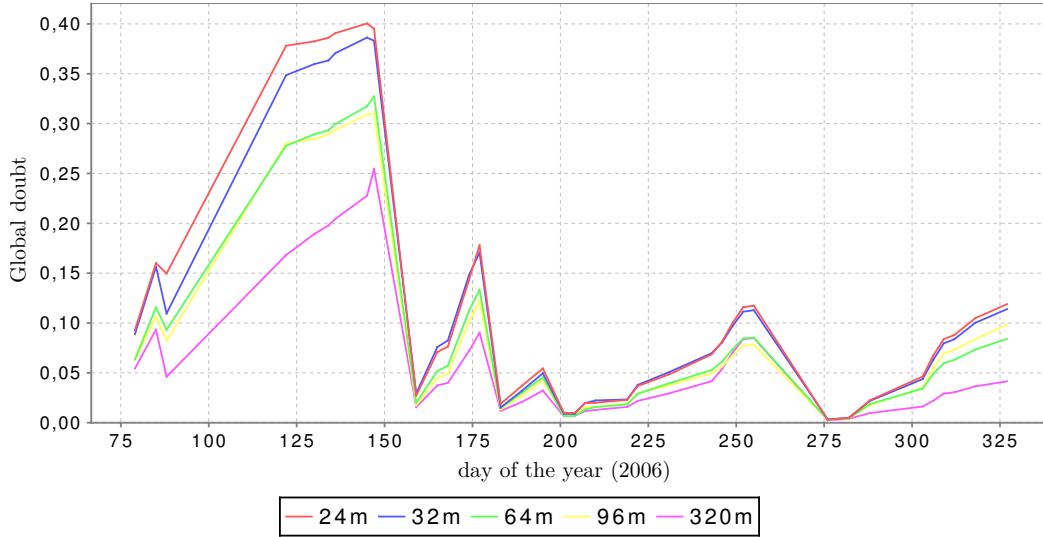


Figure 8. Evolution of the doubt on the HR classification with time.

The proposed approach fits into a wider process for exploiting the complementarity of LR and HR sensors, in order to provide the most accurate and most updated information about the observed scene. In this way, we believe this study opens up, at least, three major research directions.

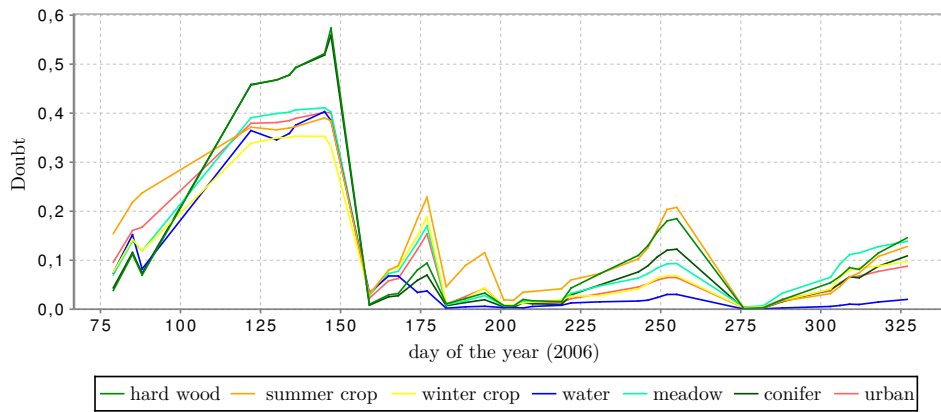
Firstly, having seen that 320 m images allowed us to develop a relevant confidence index on the classification at a higher spatial resolution, it would be interesting to study its capacity to automatically decide for the sensing of a new HR image, in order to maximise the ratio *quality of the classification over number of HR images*.

Secondly, depicted results about the confidence on the HR clusters at a time  $t$  correspond to a global evaluation of the confidence “averaged” over the cluster, and which is established through a similarity between two distribution histograms. Studying the spatial distribution of this confidence would make it possible to precisely locate the specific changing areas. This information would then make it possible to guide the collection of reference data (*e.g.*, field campaigns) by focusing the experts’ attention on these “hot spots”.

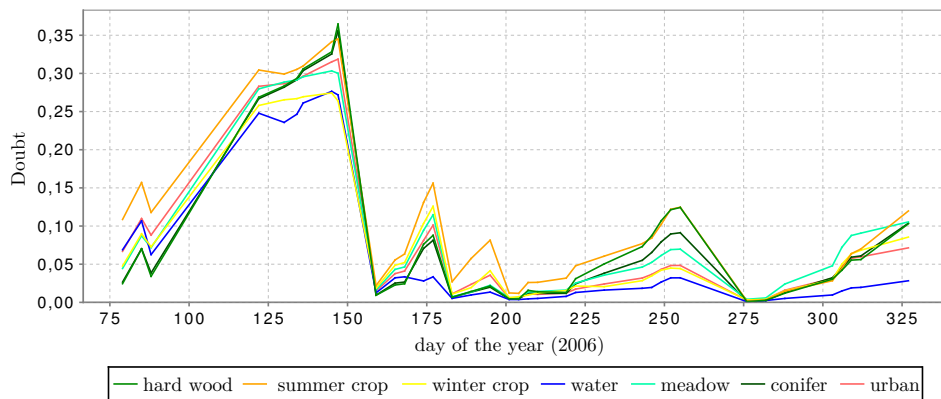
Thirdly, the comparison of distribution histograms of HR clusters into LR ones – nominal histograms, actually – has been limited to the use of the Euclidean distance. In this way, the comparison of these histograms did not take the possible proximity between the several clusters of the histograms. For example, a cluster mainly composed of broad-leaved trees is closer to one composed of conifers than another one that would be composed of water. Using a similarity measure taking into account a certain proximity between the concepts of the compared histograms – the HSB distance developed by Kurtz *et al.* (2012), for instance – would then allow us to refine the evaluation of the confidence on the classification. Globally, the study of the transformation of an histogram to another should enable to go from the reconsideration of the classification to its direct update.

### Acknowledgment

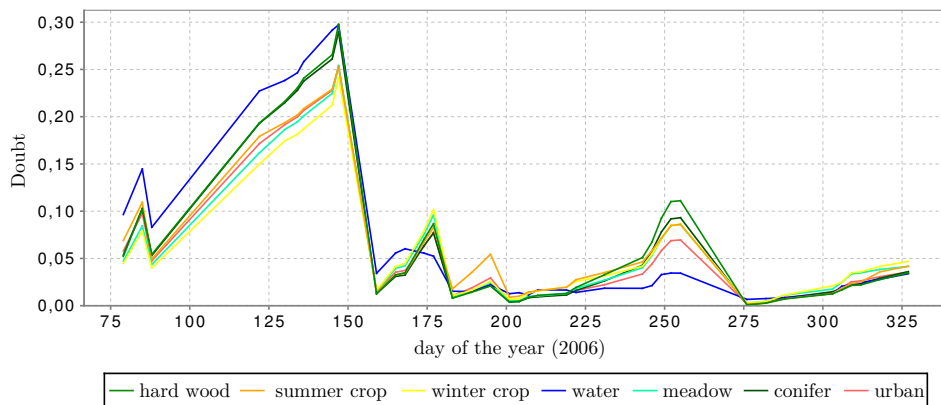
The authors would like to thank the French Space Agency (CNES) and Thales Alenia Space for supporting this work under research contract n 1520011594 and the colleagues from CESBIO (Danielle Ducrot, Claire Marais-Sicre, Olivier Hagolle and Mireille Huc) for providing the land-cover maps and the geometrically and radiometrically corrected FORMOSAT-2 images.



(a) Simulation 8 m – 24 m



(b) Simulation 8 m – 96 m



(c) Simulation 8 m – 320 m

Figure 9. Evolution of the doubt on the HR classification with time for different simulations with different low resolutions of SITS.

## References

CHEN, J., PAVLIC, G., BROWN, L., CIHLAR, J., LEBLANC, S., WHITE, H., HALL, R., PEDDLE, D., KING, D., TROFYMOW, J., SWIFT, E., DER SANDEN, J.V. and PELLIKKA, P., 2002, Derivation and validation of Canada-wide coarse-resolution leaf area index maps using high-resolution satellite imagery and ground measurements. *Remote Sensing of Environment*, **80**, pp. 165–184.

- GUPTA, R.K., 2011, Multi-Temporal and Multi-Resolution Satellite data for Urban Land Use study through Change detection techniques. *International Journal of Geomatics and Geosciences*, **2**, pp. 196–218.
- HAGOLLE, O., HUC, M., PASCUAL, D.V. and DEDIEU, G., 2010, A multi-temporal method for cloud detection, applied to FORMOSAT-2, VEN $\mu$ S, LANDSAT and SENTINEL-2 images. *Remote Sensing of Environment*, **114**, pp. 1747–1755.
- IDBRAIM, S., DUCROT, D., MAMMASS, D. and ABOUTAJDINE, D., 2009, An unsupervised classification using a novel ICM method with constraints for land cover mapping from remote sensing imagery. *International Review on Computers and Software*, **4**, pp. 165–176.
- INGLADA, J. and GARRIGUES, S., 2010, Land-cover maps from partially cloudy multi-temporal image series: optimal temporal sampling and cloud removal. In *Proceedings of the IEEE International Geoscience And Remote Sensing Symposium*, pp. 3070–3073.
- INGLADA, J., HAGOLLE, O. and DEDIEU, G., 2011, Low and high spatial resolution time series fusion for improved land cover map production.. In *Proceedings of the IEEE International Workshop on the Analysis of Multi-Temporal Remote Sensing Images*, pp. 77–80.
- KURTZ, C., PASSAT, N., GANÇARSKI, P. and PUISSANT, A., 2012, A histogram semantic-based distance for multiresolution image classification. In *Proceedings of the IEEE International Conference on Image Processing*, Sep. À paraître.
- LAPORTERIE, F. and FLOUZAT, G., 2003, The morphological pyramid concept as a tool for multi-resolution data fusion in remote sensing. *Integrated Computer-Aided Engineering*, **10**, pp. 63–79.
- LAPORTERIE-DEJEAN, F., FLOUZAT, G. and LOPEZ-ORNELAS, E., 2004, Multi-temporal and multiresolution fusion of wide field of view and high spatial resolution images through morphological pyramid. In *Proceedings of the SPIE Image and Signal Processing for Remote Sensing*, 5573, p. 52.
- MALGOUYRES, F. and GUICHARD, F., 2001, Edge Direction Preserving Image Zooming: A Mathematical and Numerical Analysis. *SIAM Journal on Numerical Analysis*, **39**, pp. 1–37.
- PETITJEAN, F., KETTERLIN, A. and GANÇARSKI, P., 2011, A global averaging method for Dynamic Time Warping, with applications to clustering. *Pattern Recognition*, **44**, pp. 678–693.
- PETITJEAN, F., KURTZ, C., PASSAT, N. and GANÇARSKI, P., 2012a, Spatio-Temporal Reasoning for the Classification of Satellite Image Time Series. *Pattern Recognition Letters*, **33**, pp. 1805–1815.
- PETITJEAN, F., INGLADA, J. and GANÇARSKI, P., 2012b, Satellite Image Time Series Analysis under Time Warping. *IEEE Transactions on Geoscience and Remote Sensing*, **50**, pp. 3081–3095.
- YANG, X. and LO, C.P., 2002, Using a time series of satellite imagery to detect land use and land cover changes in the Atlanta, Georgia metropolitan area. *International Journal of Remote Sensing*, **23**, pp. 1775–1798.